Computationally Efficient Practical Method for Solving the Dynamics of Fluid Power Circuits in the Presence of Singularities

Malysheva Iuliia, Ustinov Stanislav, Handroos Heikki

DOI: 10.1109/TMECH.2020.3038929

Computationally Efficient Practical Method for Solving the Dynamics of Fluid Power Circuits in the Presence of Singularities

Julia Malysheva, Stanislav Ustinov, and Heikki Handroos, *Member, IEEE, Member, ASME*

***Abstract*—In this paper, a practical method is proposed for the efficient solution of fluid power systems with singularities originating (in particular) from the presence in the system of small volumes. The method is based on the use of an enhanced version of the pseudo-dynamic solver (the advanced pseudo-dynamic solver), which seeks the steady-state solution of pressure building up in the small volume. This solver can be attributed to the class of explicit solvers. There are two main advantages of the proposed solver. The first is the higher accuracy and numerical stability of the solution compared with the classical pseudo-dynamic solver, owing to the enhanced solver structure and the use of an adaptive convergence criterion. The second is the faster calculation time compared with conventional integration methods such as the fourth-order Runge-Kutta method, owing to the obtained possibility of larger integration time step usage. Thus, the advanced pseudo-dynamic solver can become a preferred method in the simulation of complex fluid power circuits. Simulation results of the C code implementation confirm that the advanced pseudo-dynamic solver is better than conventional solvers for the solution of the real-time systems that include fluid power components with small volumes.**

***Index Terms*—Stiff fluid power system modeling and simulation, advanced pseudo-dynamic solver, Runge–Kutta integration, small hydraulic volumes modeling, real-time systems.**

I. Introduction

THE level of automation of mobile working machines, such as excavators, logging harvesters, or hydraulically driven cranes, as well as their complexity, have increased significantly over the past few decades. In the machine industry, this has led to emergence of novel approach in the new product development process, such as virtual prototyping [1]–[3]. Essentially, a virtual prototype of a mobile machine is the mathematical representation of all machine elements as well as their interactions. To estimate the performance of a mobile machine under development, a simulation of the virtual prototype is used. However, a major problem of virtual prototypes is often the speed of their simulation, which in particularly is related to the complexity and characteristics of the employed mathematical models. A number of studies have been dedicated to the problems of real-time [2], [4]–[6] and faster than real-time simulation [7] of the virtual prototypes of mobile machines.

J. Malysheva, S. Ustinov, and H. Handroos are with the Laboratory of Intelligent Machines, Lappeenranta-Lahti University of Technology LUT, Lappeenranta, Finland e-mail: (see iuliia.malysheva@lut.fi; stanislav.ustinov@lut.fi; heikki.handroos@lut.fi).

Manuscript received October 30, 2019.

The mechanical and fluid power components are the essential parts of any virtual prototype of mobile machines [1], [2], [8], [9] as well as various other types of mechatronic systems such as aircrafts, heavy industrial process machines, ships, off-shore cranes etc. The mathematical model of fluid power components can be presented with sets of algebraic and differential equations. By nature, such differential equations are highly nonlinear [10], and often contain singularities that make the model mathematically stiff. In particular, the stiffness in the modeling of fluid power systems is often associated with high values of the bulk modulus or with the presence of small volumes in the components of the circuit. Numerical stiffness of the model directly affects the simulation time, which is the vital aspect in real-time simulation in mechatronic applications. For instance, such problem is highlighted in [11], where authors try to solve a problem of real-time simulation of the excavator which is related to numerical stiffness in fluid power model. In order to achieve the real-time simulation speed, the model was divided into multiple sub-models for parallel execution and a local stiff integration solver was applied to the hydraulic sub-models. The same problem has been recently highlighted in a number of works dedicated to human-in-the-loop and hardware-in-the-loop systems that have fluid power components. For example in [12], authors had to simplify the fluid power model of the mechatronic component and to use third order explicit solver with small time step in order to ensure the hardware-in-the-loop real-time simulation for developed controller strategy testing. Thus, the described above mechatronic applications showed the need for the development of the method that can provide a generic practical solution to accelerate simulation of mechatronic systems including small hydraulic volumes with a minor cost in the accuracy.

In [13], Bowns and Wang were the first to formulate the mathematical stiffness problem that arises during the solution of fluid power systems in the presence of small volumes, particularly in hydraulic pipes. Physically, the mathematical stiffness occurs when the pressure is rapidly changing, owing to the low compliance of the fluid in the pipe. According to their observations, this causes the solutions of the system differential equations to decay at widely varying rates. In addition, it should be noted that the mathematical stiffness of the problem is often a local phenomenon, meaning it only occurs occasionally. Thus, if the orifice is located in the hydraulic circuit, a stiffness approaching infinity arises if the relation $\partial \Delta p / \partial Q$ is small, which is true when the volume

flow Q tends to zero. Moreover, according to [14]–[16], if the purely turbulent description of the orifice is used, the mathematical stiffness occurs also when the pressure drop Δp approaches zero.

To simulate the virtual prototype, meaning to obtain a solution for the mathematical model, numerical integration is used. The family of explicit Runge–Kutta methods that use an integration time step of fixed size are well established in the solution of systems of ordinary differential equations (ODEs). However, it was shown in [17] that numerical integrators based on explicit Runge–Kutta methods are not A-stable (the numerical stability of the method is not guaranteed for any integration step size), which is apparently why they are not very efficient on stiff problems unless a very small integration time step is used. At the same time, integrators based on implicit methods have established themselves as A-stable or even L-stable, which allows the accurate solution of such problems. However, implicit methods are much more computationally expensive. In general, they involve solving a nonlinear system of algebraic equations at each time step. This in turn requires a modified Newton iteration scheme, which includes the calculation of iteration matrix of the form $(\mathbf{I} - \Delta t\beta_0\mathbf{J})$, where $\mathbf{I}$ is the identity matrix, $\mathbf{J}$ is the Jacobian and $\Delta t\beta_0$ is a scalar, and also further its factorization. The iteration scheme is repeated until a convergence criterion is reached [18]. Due to such iteration scheme the amount of computations can vary from step to step which can result in simulation time overflows. Thus, implicit methods cannot be used directly in real-time applications. In contrast to implicit methods the previously mentioned explicit methods can ensure a constant simulation time in time-critical real-time applications.

On the other hand, the integration in fluid power systems can be performed with the help of special solvers [19]. To overcome the stiffness of differential equations in fluid power systems with small volumes, a pseudo-dynamic solver was proposed by Åman and Handroos [20]–[22]. This solver can be related to the class of explicit solvers. The goal of the solver algorithm was to increase the accuracy and to reduce the computational time for the simulation of stiff fluid power circuits. The proposed solver was based on the assumption that if the considered volume was small enough, the build-up pressure can be substituted by a steady-state pressure. The goal was achieved by implementing an iterative technique with substituting the small volume with a volume that is large enough to obtain a numerically stable response in pressure. The solver showed its applicability at relatively large integration time steps, whereas conventional stiff models used very small time steps to simulate the circuit without numerical instability, affecting the computational time of the simulation. However, in their work, only a short-term simulation (about 2 seconds) with predefined inputs was considered, which did not give a full picture of the solver characteristics.

Another interesting method of solving pressures in small volumes in fluid power systems was recently introduced by Kiani-Oshtorjani et al. [23] and further applied for the mechatronic system accelerated simulation in [6], [24]. The proposed method was based on singular perturbation theory. The modified version of this theory was used for the algorithm. The main principle of the algorithm was the replacement of stiff differential equation of pressure by the algebraic equation in accordance with singular perturbation theory. The replacement of the differential equation allows a numerically stable response of the pressure to be achieved at different integrator time steps. Consequently, the time step of the integration can be increased without significant losses in calculation accuracy, which allows the method to be implemented in real-time simulations. Moreover, in the works [6], [24] Rahikainen et al. emphasized that the fluid power system due to its stiffness needs much smaller integration time step than the multibody system during the coupled simulation which sufficiently increases the simulation speed of the whole mechatronic system. However, the method based on singular perturbation theory may have limited applicability, such as it only can be applied under certain conditions of the system when the boundary layer is exponentially stable [23].

The objective of the present research is to develop a method that quickly finds an accurate and numerically stable solution for stiff fluid power circuits with increased modeling accuracy, to accelerate their simulation. For this purpose, the classical pseudo-dynamic solver [20]–[22] was selected as a basis for the research. In this work, the characteristics of the pseudo-dynamic solver are studied in more detail by applying long-term simulation together with random inputs to the test fluid power circuits. Based on the obtained results the new Advanced pseudo-dynamic solver (AdvPDS) of the enhanced structure is proposed. The developed solver provides a fast and accurate solution of more complex fluid power circuits in the presence of singularities caused by small volumes.

The structure of the present research paper is organized as follows. Section II describes the systems under investigation. Section III contains a brief description of the classical pseudo-dynamic solver. The development and features of the AdvPDS are described in Section IV. Results and discussion are presented in Section V, where the results obtained by the developed method are compared with the results obtained using conventional way models of stiff fluid power circuits and classical pseudo-dynamic solver. Finally, Section VI contains the conclusion of present research.

II. Fluid power circuit modeling

Fluid power circuit modeling can be approached from the point of view of lumped fluid theory [9], [25]. According to this theory, any fluid power circuit can be considered as a number of separate volumes with evenly distributed pressures. The volumes are separated by throttles and orifices that create pressure drops in the fluid when passing through them. In turn, the pressure drop together with orifice geometrical parameters are used for the volume flow calculation. Finally, pressure built up in each volume can be calculated using a continuity equation that relates the effective bulk modulus with respect to the considered volume and the difference between inlet Q_{in} and outlet Q_{out} volume flows [10], [26].

A. Circuit 1: two-way flow control valve

The first system under investigation is a two-way flow control valve. The fluid power circuit related to the system

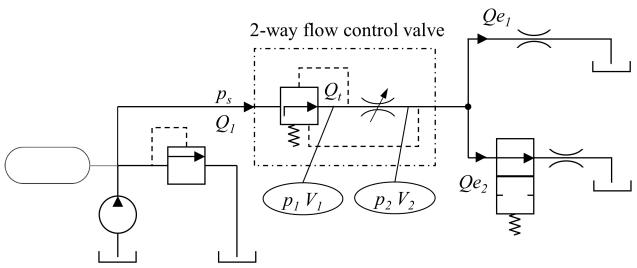

Fig. 1. Schematic representation of Circuit 1

is schematically depicted in Fig. 1. The circuit consists of a pressure power source, two-way flow control valve, orifice, and 2/2 directional control valve. A two-way flow control valve consists of two components: pressure compensator and control throttle. The volume between the pressure compensator and control throttle is assumed to be a small volume, the presence of which increases the stiffness of the system. The power source is assumed an ideal pressure source with constant pressure. It is composed of a hydraulic accumulator, pump, pressure relief valve, and tank. To reach the tank, hydraulic fluid flow passes through a two-way control valve and two orifices after the valve. One of the orifices is an ordinary sharp-edged orifice, whereas the other is a 2/2 directional control valve, the opening of which can be controlled by signal U_d. Pressure in the system can be integrated from the following continuity equations:

$$\dot{p_1} = \frac{B_e}{V_1}(Q_1 - Q_t) \tag{1}$$

$$\dot{p_2} = \frac{B_e}{V_2}(Q_t - Q_{e1} - Q_{e2}) \tag{2}$$

where B_e is the oil effective bulk modulus, V_1 and V_2 are pipeline volumes, where V_1 is a small volume, Q_1 and Q_t are volumetric flows through the pressure compensator and control throttles, and Q_{e1} and Q_{e2} are orifice and directional control valve volume flows, respectively. Volume flows Q_1 and Q_t can be obtained as follows:

$$Q_1 = K\sqrt{|p_s - p_1|}sign(p_s - p_1) \tag{3}$$

$$Q_t = k_t\sqrt{|p_1 - p_2|}sign(p_1 - p_2) \tag{4}$$

where p_s is the supply pressure, K and k_t denote the semi-empirical flow coefficients for the pressure compensator throttle and for the control throttle, respectively. Both coefficients can be integrated from the following differential equations:

$$\dot{K} = \frac{C_5 - p_1 + p_2 - (C_1 + C_2(p_s - p_1))K}{C_3} \tag{5}$$

$$\ddot{k_t} = (U_e - C_9)C_6C_7^2 - 2\dot{k_t}C_8C_7 - k_tC_7^2 \tag{6}$$

where U_e is the signal applied to control throttle (opening), C_1, C_2, C_3, C_5, C_6, C_7, C_8, C_9 are empirical constants [27]. Volume flows Q_{e1} and Q_{e2} are obtained according to the following flow equations:

$$Q_{e1} = k_1\sqrt{p_2 - p_t} \tag{7}$$

TABLE I
CIRCUIT 1 PARAMETERS

B_e	$1.5{\cdot}10^9$ Pa	C_1	$4.65{\cdot}10^7$
V_1	$1.0{\cdot}10^{-5}$ m^3	C_2	$-1.79{\cdot}10^4$
V_2	$1.0{\cdot}10^{-3}$ m^3	C_3	$4.0{\cdot}10^{11}$
k_1	$5.62{\cdot}10^{-7}$	C_5	$1.02{\cdot}10^6$
k_2	$5.73{\cdot}10^{-7}$	C_6	$5.26{\cdot}10^{-7}$
p_t	0 Pa	C_7	200
K	$0.05{\cdot}10^{-9}$	C_8	0.45
k_t	$1.0{\cdot}10^{-7}$	C_9	1.2

$$Q_{e2} = k_2\sqrt{p_2 - p_t} \tag{8}$$

where k_1 and k_2 are semi-empirical flow coefficients for the orifice and directional control valve, and p_t is the tank pressure. The initial values and constants of the system described in following equations are shown in Table I. To analyze the mathematical stiffness of the developed model of Circuit 1, its state-space representation should be derived. If we assign the state and input vectors as $\mathbf{x} = [x_1\ x_2\ x_3\ x_4\ x_5]^T = [p_1\ p_2\ K\ k_t\ \dot{k_t}]^T$ and $\mathbf{u} = [u_1\ u_2\ u_3]^T = [p_s\ U_e\ \varepsilon]^T$, respectively, then the state equations can be written as follows:

$$\begin{aligned}
\dot{x_1} &= \frac{Be}{V_1}(x_3\sqrt{u_1 - x_1} - x_4\sqrt{x_1 - x_2}) \\
\dot{x_2} &= \frac{Be}{V_2}(x_4\sqrt{x_1 - x_2} - k_1\sqrt{x_2} - u_3(k_2\sqrt{x_2})) \\
\dot{x_3} &= \frac{1}{C_3}(x_2 - x_1 + C_2x_1x_3 - C_2x_3u_1 - C_1x_3 + C_5) \\
\dot{x_4} &= x_5 \\
\dot{x_5} &= C_6C_7^2u_2 - 2C_7C_8x_5 - C_6C_7^2C_9 - C_7^2x_4
\end{aligned} \tag{9}$$

The obtained state-space representation (9) is a multi-input multi-output nonlinear model, where ε is the parameter that describes the binary input of the 2/2 directional control valve. If ε is equal to 0 the valve is closed and the term $k_2\sqrt{x_2}$ will be also equal to zero.

One way to detect the stiffness in the problem is to estimate the dominant eigenvalues of its Jacobian directly. In linear system theory, the eigenvalues of the system Jacobian describe the behavior modes inherent in the model. In nonlinear systems, eigenvalues and eigenvectors are time-varying. Nevertheless, it is possible to apply this approach to nonlinear problems through model linearization. Linearization means that constantly differentiating nonlinearities are linearly approximated about their operating points. As the linearized solutions can be considered as a good approximation of nonlinear system solutions about the operating point, the observations obtained locally can be generalized to the rest of the system. Further, to simplify the model we also assume that flows through the compensator and control throttles have constant coefficients K and k_t, which is often valid and frequently employed in fluid power systems design. The Jacobian of the system can be calculated as

$$\mathbf{J} = \frac{\partial \mathbf{F}}{\partial \mathbf{x}}\bigg|_{\mathbf{x}=\bar{\mathbf{x}},\mathbf{u}=\bar{\mathbf{u}}} \tag{10}$$

where $\mathbf{F}$ is the left-hand side of the first and second equation of (9) , $\mathbf{x}$ is the model state vector, $\mathbf{u}$ is the model input vector, and

$(\bar{\mathbf{x}}, \bar{\mathbf{u}})$ is the operating point. The Jacobian for the considered system can be written as follows:

$$\begin{bmatrix} -\frac{Be}{2V_1}\left(\frac{K}{\sqrt{u_1-x_1}}+\frac{k_t}{\sqrt{x_1-x_2}}\right) & \frac{Be}{2V_1}\frac{k_t}{\sqrt{x_1-x_2}} \\ \frac{Be}{2V_2}\frac{k_t}{\sqrt{x_1-x_2}} & \frac{Be}{2V_2}\left(\frac{k_1+k_2}{\sqrt{x_2}}+\frac{k_t}{\sqrt{x_1-x_2}}\right) \end{bmatrix} \quad (11)$$

To characterize the level of numerical stiffness of the model, we employ a condition number of the Jacobian, which, according to numerical analysis theory, can be written as

$$\kappa(\mathbf{J}) = \frac{|\lambda_{max}(\mathbf{J})|}{|\lambda_{min}(\mathbf{J})|} \quad (12)$$

where $\lambda_{max}(\mathbf{J})$ and $\lambda_{min}(\mathbf{J})$ are the maximum and minimum eigenvalues of the Jacobian, respectively, which for $\mathbf{J} \in \mathbf{M}_{n\times n}$ should satisfy $|\mathbf{J}-\lambda\mathbf{I}| = \mathbf{0}$, where $\mathbf{I}$ is the identity matrix. The condition number shows how much the eigenvalues of the system differ, i.e., small values of κ show that the problem is well-conditioned, whereas large values of κ indicate the ill-conditioned problem and the system can be considered as stiff. The condition number can be determined for the certain configuration of the system. This means that the Jacobian should be calculated in the operating point $(\bar{\mathbf{x}}, \bar{\mathbf{u}})$. To define such a point, the physical characteristics of the state variables should be considered. Thus, the following physical restrictions should be imposed on the state variables and inputs: $x_1, x_2 > 0, x_3 \in [0, 10^{-6}], x_4 > 10^{-7}, u_1 > 0, u_2 \in [0, 10], u_3 \in \{0, 1\}$. Under the restrictions, the operating point can be chosen as $\mathbf{x} = [198 \cdot 10^5,\ 1.5 \cdot 10^5,\ 10^{-6},\ 10^{-7},\ 0]^T$ and $\mathbf{u} = [200 \cdot 10^5,\ 6]^T$. Note, that x_1 and x_2 are calculated from first and second equation of (9) by substituting x_3 and x_4 with the constant values and assuming that all the rates are equal to zero.

At this point, let us consider the two cases. In the first case $V_1 = 10^{-3}\ m^3$, i.e., the volume between compensator and control throttle is quite large. The condition number of (11) in the chosen operating point for this case is $\kappa = 1.28$. In the second case the volume is reduced to $V_1 = 10^{-5}$ m^3 and the corresponding condition number becomes as large as $\kappa = 77.81$. Analyzing the system Jacobian (11), this effect can be seen through the fact that the small volume V_1 appears in the denominator of the Jacobian elements and, thus, makes the eigenvalues differ significantly in magnitude and the mathematical model (9) become numerically stiff.

B. Circuit 2: pressure compensating proportional valve

The next fluid power system considered here has a more complex structure and is more practical. The system is the part of the fluid power circuit of the hydraulic crane PATU 655, the modeling of which was considered in [4], [7]. The considered part includes a differential cylinder with an attached sliding load, a 4/3-proportional directional valve with a pressure compensator, and a constant pressure pump. In the system, the small volume appears between the directional valve and pressure compensator. In Fig. 3 the small volume and the pressure developing within it are denoted by V_3 and p_3, respectively. The system is controlled through the voltage signal U supplied to the valve solenoids:

$$\ddot{U}_s = K_v\omega_n^2 U - 2\zeta\omega_n\dot{U}_s - \omega_n^2 U_s \quad (13)$$

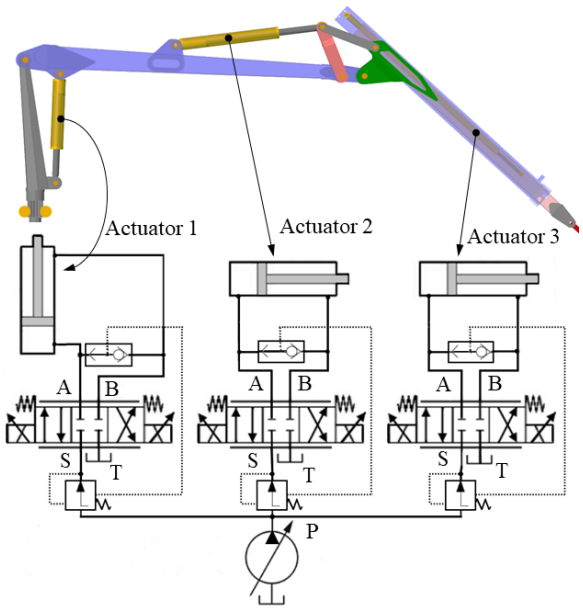

Fig. 2. Hydraulic crane PATU 655 actuated by the fluid power system

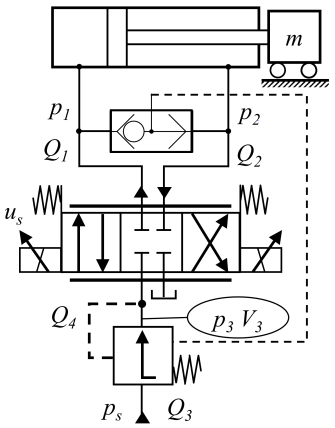

Fig. 3. Schematic representation of Circuit 2

where K_v is the valve gain, U_s is the signal proportional to the valve spool displacement, ζ is the valve damping ratio, and ω_n is the natural angular frequency. The volume flow rates model of the 4/3-proportional directional valve using turbulent orifice model with triangular groove cross-section can be presented as

$$\begin{aligned} Q_1 = & \\ & \begin{cases} C_\nu(U_s - U_{db})^2 sign(p_s - p_1)\sqrt{|p_s - p_1|}, U_s \geq U_d \\ C_\nu(U_s - U_{db})^2 sign(p_1 - p_t)\sqrt{|p_1 - p_t|}, U_s \leq -U_d \\ 0, \text{otherwise} \end{cases} \\ Q_2 = & \\ & \begin{cases} -C_\nu(U_s - U_{db})^2 sign(p_2 - p_t)\sqrt{|p_2 - p_t|}, U_s \geq U_d \\ -C_\nu(U_s - U_{db})^2 sign(p_s - p_2)\sqrt{|p_s - p_2|}, U_s \leq -U_d \\ 0, \text{otherwise} \end{cases} \end{aligned} \quad (14)$$

In (14), C_ν is the flow constant that accounts for cross-sectional areas of the valve orifices, U_{db} is the dead band

voltage of the valve, and p_1, p_2, p_s, and p_t are the pressures in two cylinder chambers, the supply pressure, and the pressure in the tank, respectively. In this work, the directional valve is assumed ideal, such that there are no internal leakages. The volume flow Q_3 related to the pressure compensator is modeled using the semi-empirical approach developed in [27]:

$$\begin{aligned} Q_3 &= K\sqrt{p_s - p_3}, \\ \dot{K} &= \frac{1}{C3}(C5 - p_3 + p_{shuttle} - (C1 + C2(p_s - p_3))K) \end{aligned} \tag{15}$$

where $p_{shuttle} = \max(p_1, p_2)$ is the output of the shuttle valve (Fig. 3). The volume flow Q_4 between valve and pressure compensator can be considered as equal to Q_1 if $U_s \geq U_{db}$, and equal to $-Q_2$ if $U_s \leq -U_{db}$.

According to Newton's second law, the equation of motion of a hydraulic cylinder can be written as

$$m\ddot{x}_p = p_1 A_1 - p_2 A_2 - F_f \tag{16}$$

where $\ddot{x}_p$ is the acceleration of the cylinder piston, m is the load mass, p_1 and p_2 are the pressures in the cylinder chambers, A_1 and A_2 are the piston-side and rod-side areas, respectively, and F_f is the cylinder friction force. In turn, the friction formed in the cylinder can be represented using the LuGre friction model [28], [29]:

$$\begin{cases} F_f = \sigma_0 z + \sigma_1 \dot{z} + k_\nu \dot{x}_p \\ \dot{z} = \dot{x}_p - \dfrac{|\dot{x}_p|}{g(\dot{x}_p)} z \\ g(\dot{x}_p) = \dfrac{1}{\sigma_0}\left(F_C + (F_{st} - F_C)\exp\left(-\left(\dfrac{\dot{x}_p}{v_{st}}\right)^2\right)\right) \end{cases} \tag{17}$$

where σ_0 is the flexibility coefficient, σ_1 is the damping coefficient, k_ν is the friction coefficient, F_C is the Coulomb friction, F_{st} is the Stribeck friction, and v_{st} is the Stribeck velocity. More specifically, z represents the non-measurable internal state, $g(\dot{x}_p)$ describes the friction behavior during constant velocity motion, and $k_\nu \dot{x}_p$ is the viscous friction.

The internal leakage flow Q_{Li} (m^3/s) between the cylinder chambers can be approximated as

$$Q_{Li} = L_i(p_1 - p_2) \tag{18}$$

where L_i is the laminar leakage flow coefficient.

The pressures that are building up in the circuit can be calculated from

$$\begin{cases} \dfrac{V_1}{\beta_{e1}}\dot{p}_1 = Q_1 - A_1\dot{x}_p + Q_{Li} \\ \dfrac{V_2}{\beta_{e2}}\dot{p}_2 = -Q_2 + A_2\dot{x}_p - Q_{Li} \\ \dfrac{V_3}{\beta_{e3}}\dot{p}_3 = Q_3 - Q_4 \end{cases} \tag{19}$$

where the chamber volumes V_1 and V_2 are calculated as

$$\begin{cases} V_1 = A_1 x_p + V_{01} \\ V_2 = A_2(H - x_p) + V_{02} \end{cases} \tag{20}$$

Here H is the cylinder stroke and V_{01}, V_{02} are the dead volumes connected to the respective ports. In (19), the compressibility of hydraulic oil is accounted for by the effective bulk modulus β_{ei} ($i = 1, 2, 3$). The effective bulk modulus for each part of the system is calculated regarding the local pressure using the empirical formula [30]:

$$\beta_{ei} = a_1 E_{max} \log\left(a_2 \frac{p_i}{p_{max}} + a_3\right) \tag{21}$$

where E_{max} denotes the maximum bulk modulus of the oil, p_{max} is the maximum pressure in the system, and a_i ($i = 1, 2, 3$) are the empirical constants. The values of parameters used in the hydraulic model described in this section are listed in Table II.

TABLE II
CIRCUIT 2 PARAMETERS

m	210 kg	L_i	$1.72{\cdot}10^{-13}$ m^3/sPa
A_1	$8.04{\cdot}10^{-4}$ m^2	$C1$	$4.65{\cdot}10^{7}$
A_2	$4.24{\cdot}10^{-4}$ m^2	$C2$	$-1.79{\cdot}10^{4}$
V_{01}	$1.0{\cdot}10^{-3}$ m^3	$C3$	$4.0{\cdot}10^{11}$
V_{02}	$1.0{\cdot}10^{-3}$ m^3	$C5$	$8.0{\cdot}10^{5}$ Pa
C_ν	$2.31{\cdot}10^{-9}$ $m^3/sV\sqrt{Pa}$	V_3	$1.0{\cdot}10^{-5}$ m^3
H	1 m	U_{db}	2 V
p_s	$1.4 \cdot 10^{7}$ Pa	E_{max}	$1.8{\cdot}10^{9}$ Pa
p_t	$9.0 \cdot 10^{5}$ Pa	p_{max}	$2.8{\cdot}10^{7}$ Pa
K_v	$9.9{\cdot}10^{-1}$	σ_0	$3.2{\cdot}10^{2}$ N/m
ω_n	$3.31{\cdot}10^{2}$ rad/s	σ_1	6.3 Ns/m
ζ	$6.2{\cdot}10^{-1}$	k_ν	$1.28{\cdot}10^{3}$ Ns/m
a_1	0.5	F_C	$2.15{\cdot}10^{6}$ N
a_2	90	F_{st}	$1.13{\cdot}10^{10}$ N
a_3	3	v_{st}	$3.47{\cdot}10^{2}$ m/s

Equations (13)–(21) make up the mathematical model of Circuit 2. The presence in the model of the pressurized small volume makes the mathematical equations stiff and, hence, computationally costly.

III. PSEUDO-DYNAMIC SOLVER OF PRESSURE IN SMALL VOLUMES

The main idea of the pseudo-dynamic solver proposed in [16] lies in searching for a steady-state solution for pressures related to small volumes in fluid power circuits. At the same time, the pressures built up in larger volumes are solved with the conventional integration algorithms. Thus, the pseudo-dynamic solver includes two integration loops: the main loop, which contains algebraic and differential equations related to larger volumes, and the inner loop. The inner loop, using artificially enlarged fluid volume, searches for the steady-state value of pressure passing by the transition process of pressure formation. The steady-state value of pressure is sought out during the single time step of the main loop.

The pressure inside the inner loop can be calculated from the classical continuity equation using artificially enlarged fluid volume as follows:

$$\dot{p} = \frac{B_e}{V_{pseudo}}(Q_{in} - Q_{out}) \tag{22}$$

where V_{pseudo} is the artificial pseudo-volume, B_e is the effective bulk modulus of the oil, and Q_{in} and Q_{out} are the inlet and outlet volume flows, respectively. According to [21], the pseudo-volume is recommended to be set at least 10 times

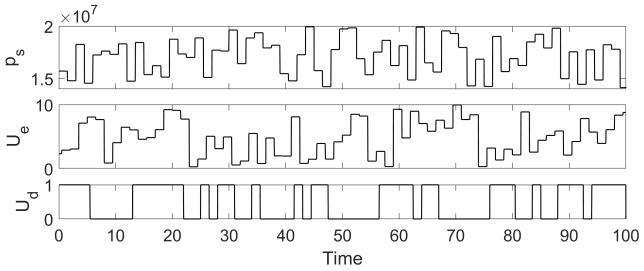

Fig. 4. Input signals for Circuit 1

higher than the actual volume. Inlet and outlet volume flows can be expressed as a function of pressure drop as follows:

$$Q = f(\Delta p) \tag{23}$$

The integration of differential equation 22 inside the inner loop occurs by using an explicit fixed-step fourth-order Runge–Kutta integration routine with independent sufficiently small time step t_i. The integration routine continues until the convergence criterion is reached. The criterion is a predefined user parameter, which represents the first derivative of the pressure. It is important to note that the activation of the inner loop suspends the main loop until the steady-state pressure value is found.

IV. Development of the AdvPDS with adaptive criterion

To study the characteristics of the pseudo-dynamic solver described in Section III, a simple fluid power system (Circuit 1) was employed. Circuit 1 is a more complicated variant of the fluid power circuit used in [21]. The three random signals in the form of pseudo-random multilevel signals (PRMSs) were supplied as the inputs: supply pressure p_s in the range 14–20 MPa, control voltage to the control throttle U_e in the range -10 to +10 V, and directional valve control signal U_d, which took either 1 when it is open or 0 when it is closed (Fig. 4). The signals were supplied asynchronously with a period of 0.5 s. The system was simulated using a conventional fourth-order Runge–Kutta integrator with sufficiently small time step of 10^{-6} s for 100.5 s. During the simulation, the small volume V_1 is equal to 10^{-5} m^3. The simulation took about 5 hours using the following simulation environment: MATLAB 2018b, Intel Core i5-4590 3.30 GHz with 16 GB of RAM, running OS Windows 7 64-bit. The fourth-order Runge–Kutta solver is considered further in this work as a reference solver and the solutions obtained with its help thus also considered as a reference. The solution for the pressure p_1 was obtained under such conditions and was used as a reference in the case of Circuit 1.

The classical pseudo-dynamic solver (described in Section III) was introduced in the same simulation using recommended parameters. Unfortunately, it could not achieve a stable solution compromising it's speed and accuracy. While studying the reasons for such a behavior, it was discovered that the solver becomes numerically unstable in areas of sudden pressure change owing to fixed Q_{out} in (22) during integration in the inner loop. To stabilize the numerical solution it was decided

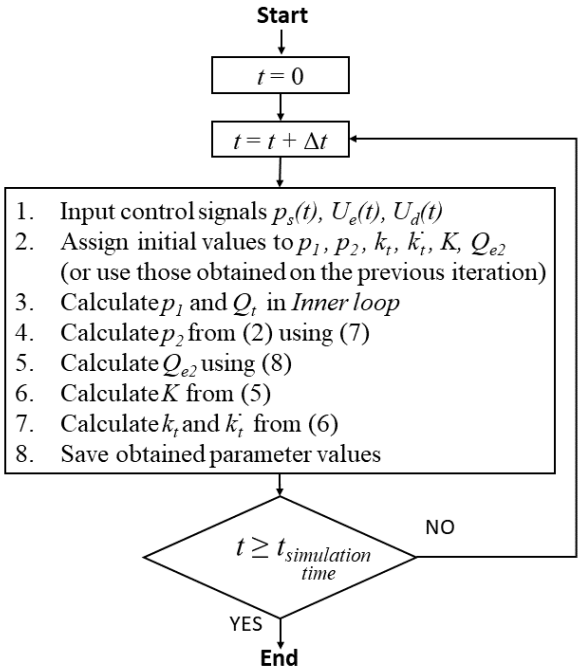

Fig. 5. Main loop sequence for Circuit 1

to move the calculation of Q_{out} into the inner loop. Thus, in terms of Circuit 1, the pressure build-up in the small volume (1) as well as inlet and outlet volume flows described by (3) and (4), respectively, are calculated in the inner loop. However, it was also found that the calculation of other system elements such as K and k_t inside the inner loop does not have much of an effect on the solution accuracy, moreover it makes the simulation longer. These findings formed the basis for the AdvPDS.

Further, in order to describe the operating principle of the AdvPSD Circuit 1 is used as an implementation example. Similar to the classical pseudo-dynamic solver, the AdvPDS consists of two integration loops.The main loop (Fig. 5) begins with the reading of the current control signals $p_s(t)$, $U_e(t)$, and $U_d(t)$. Then, the initial values of pressures p_1 and p_2, as well as current control signal $p_s(t)$ are sent to the inner loop, and the inner loop starts to execute. Initial values of pressures, volume flows, and flow coefficients are used in the main and inner loops during the first iteration. In the following iterations, the pressure and flow values are updated every time step. The inner loop (Fig. 6) first saves the previous value of the pressure p_1. The value of pressure should be saved every iteration to calculate the rate of pressure change between the adjacent iterations. The running of the inner loop occurs at its own integration time step Δt_i that may differ from the main loop time step Δt. It is important to note that the main loop is suspended during the execution of the inner loop. Further calculation of the volume flows through the pressure compensator ($Q_{1pseudo}$) and control throttle (Q_t) is performed only inside the inner loop using equations (3) and (4), respectively. Next, the pressure p_1 is integrated from (1). Note, that the small volume from (1) is substituted with the pseudo-volume as in (22). Obtained pressure value is used

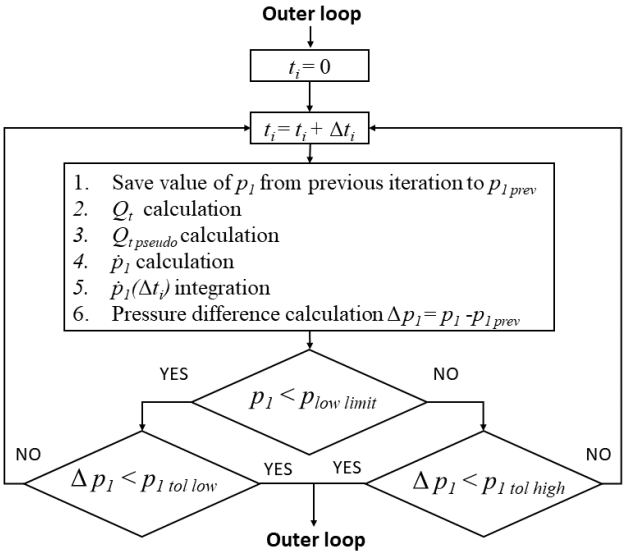

Fig. 6. Inner loop sequence for Circuit 1

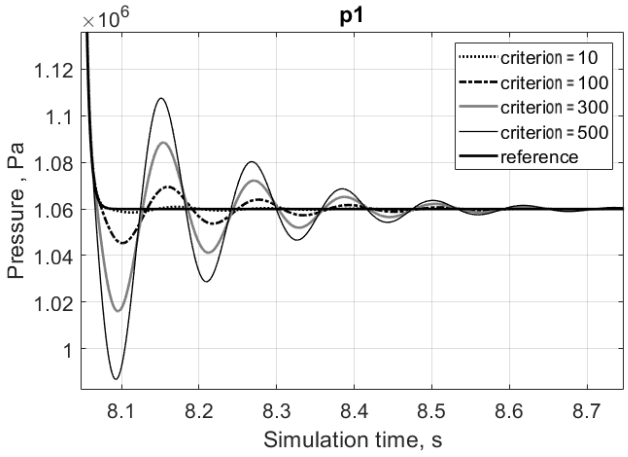

Fig. 7. Effect of the criterion value on the low-pressure calculation using the AdvPDS

to calculate the pressure difference, which is further compared to the convergence criterion value.

In the classical pseudo-dynamic solver the single convergence criteria was used. The criteria was based on the rate of pressure change between the iterations in the inner loop. The rate of pressure change between the iterations Δp_1 can be written as:

$$\Delta p_1 = p_1 - p_{1prev} \tag{24}$$

where p_1 is the pressure from the current iteration, and p_{1prev} is the pressure from the previous iteration of the inner loop. The rate of pressure change is compared with the convergence criterion value to detect the beginning of the steady-state process of the pressure. The captured steady-state value is further passed to the main loop.

The effect of the single criterion value in the inner loop of the AdvPDS on the solution accuracy was also studied. It was discovered that applying a smaller convergence criterion in the inner loop produces a more numerically stable result when the pressure approaches its lower values during the simulation. In Fig. 7 the effect of the criterion value on the calculation of the low pressures using the AdvPDS is shown. At the same time, it was noticed that the computational time of the simulation increases with the criterion decrease owing to the large number of iterations performed inside the inner loop. Thus, the adaptive convergence criterion was proposed. The idea behind the adaptive criterion is that depending on the pressure level, the criterion with the most suitable time-efficient and numerically stable effect on the pressure is automatically selected during the fluid power circuit simulation. According to Fig.6 when the pressure difference between the iterations Δp_1 is calculated using (24) the current pressure level p_1 is compared to assigned low-pressure level $p_{low\ limit}$. If the current pressure level is low the smaller criteria is used, i.e. inner loop continues to iterate until the change in the pressure is less then $p_{1\ tol\ low}$. If $p_1 > p_{low\ limit}$ the inner loop proceeds with criteria $p_{1\ tol\ high}$. In other words, at low pressure levels in the system, the smaller criterion is implemented to achieve a more numerically stable result. At pressure levels higher than the low-pressure limit, the bigger criterion is used to reduce the computational time of the simulation. The low-pressure level was defined experimentally and for both Circuits 1 and 2 it was 22 bar. Both criteria have to be predefined by the user before the simulation, based on the recommendations given further in this work. When the criterion is satisfied, the value of pressure p_1 and flow Q_t are updated for subsequent calculations in the main loop. The main loop further updates the pressure p_2, and flows Q_{e1} and Q_{e2} according to (2), (7), and (8), respectively. Then calculation of flow coefficients (K and k_t) according to equations (5) and (6) is performed. The next iteration of the main loop begins at the next time step Δt. The process continues for all specified simulation time.

V. Results and Discussion

In this section, the results of the simulation of the two fluid power circuits described in Section II are presented. The results are represented through a comparison of the responses of the considered fluid power circuits obtained using the reference solver and the AdvPDS. The results demonstrate the features of the proposed method and its advantages compared with the traditional method of fluid power system modeling and simulation.

A. Circuit 1 simulation

Circuit 1 was simulated for 100.5 s using the AdvPDS and the reference solver with the inputs described in Section IV. The presence of the small volume ($V_1 = 10^{-5}$ m^3) in the circuit between the pressure compensator and control throttle increased the stiffness of the whole system, and also determined the selection of the integration time step for the reference solver. The integration time step of the reference system was set to the largest possible value of 1×10^{-6} s, at which the solution for the pressure appeared numerically stable.

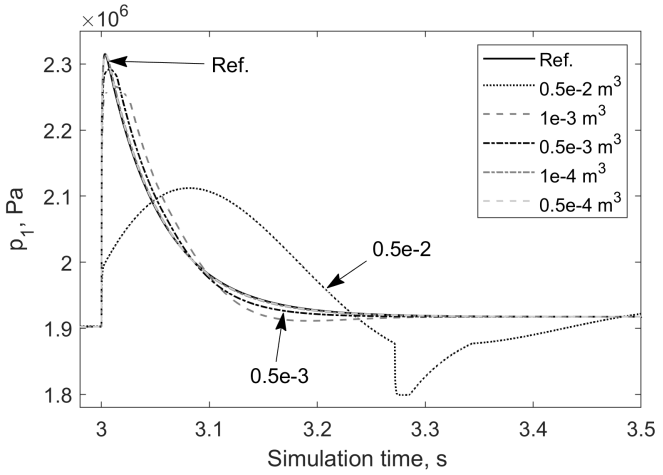

Fig. 8. Sensitivity analysis of p_1 solution to the changes in V_{pseudo}

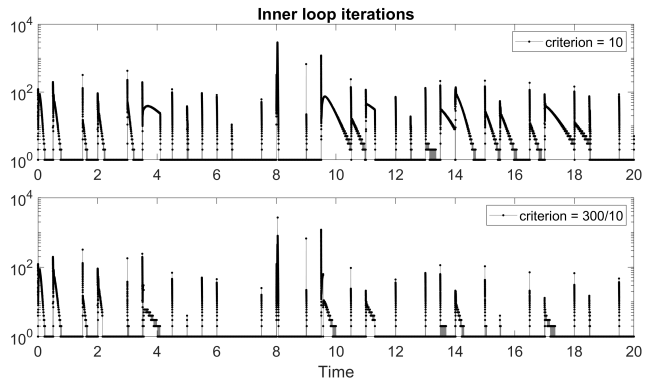

Fig. 9. Number of iterations performed by the AdvPDS in the inner loop during the first 20 s of the simulation with 10 (upper plot) and 300/10 (lower plot) criteria

The use of the AdvPDS with Circuit 1 allows the stiffness of the system to be reduced owing to substitution of the small volume by the larger artificial volume. In the mathematical model of Circuit 1 the artificial volume V_{pseudo} substitutes the real volume V_1 in (1). This volume directly affects the resulting pressure p_1. In order to analyse how the size of the artificial volume affects the respective pressure solution a simple sensitivity analysis was carried out. The sensitivity analysis was performed in a way that Circuit 1 is simulated five times with the same input signals and parameter values except for the pseudo-volume value. In the experiment V_{pseudo} took the following values: 0.5×10^{-2} m^3, 1×10^{-3} m^3, 0.5×10^{-3} m^3, 1×10^{-4} m^3, and 0.5×10^{-4} m^3. The upper bound of the pseudo-volume range was limited by the system stability while holding the condition $\Delta t_i = 10^{-5}$ s. In Fig. 8. the results of five simulations are presented. For better visibility only short range of the simulation time is shown in the figure. It should be noted that the biggest difference in the pressure solutions of five simulations is observed in the transition areas, when one of the control signals was changed. One of such areas is shown in Fig. 8. It can be seen from the figure that the four solutions that refer to the smaller pseudo-volumes are rather close to the reference one. Only the solution obtained using the biggest volume 0.5×10^{-2} m^3 compromised the accuracy. Taking into account the obtained results the artificial volume was set to $V_{pseudo} = 1 \times 10^{-3}$ m^3. On the one hand, the pseudo-volume of this size ensured quite high accuracy of the solution. On the other hand, it allowed the integration time steps for the main and inner loops to be increase significantly and to be set to the values of 10^{-4} s and 10^{-5} s, respectively.

As it was previously mentioned, the number of iterations performed in the inner loop at each time step has also a direct effect on the simulation time. The transition process is more oscillatory, and the larger the pressure changes, the more iterations are performed in the inner loop. At the same time, the number of iterations is dependent on the chosen convergence criterion. It was found experimentally that the larger criterion is associated with the smaller number of iterations. Thus, to speed up the simulation of the AdvPDS-based system, the adaptive convergence criterion 300 Pa/10 Pa was selected based on experimental results. In Fig. 9, the number of iterations performed by the AdvPDS using a single convergence criterion in comparison with the use of the adaptive criterion is shown for the first 20 seconds of the simulation. It can be seen from the figures that the AdvPDS executed a higher number of iterations in transition areas with the single criterion than with the adaptive criterion, which resulted in a shorter simulation time.

Figure 10 shows the pressure responses p_1 of Circuit 1, obtained with the reference solver and the AdvPDS. One can observe that the two curves are highly coincident with each other. Now the high accuracy of the AdvPDS-based system was also achieved on the low-pressure areas. The accuracy of the system was represented through root-mean-square error (RMSE). The overall error was RMSE = $1.12 \cdot 10^4$Pa, which is insignificant for such high pressure levels in the system.

Thus, the use of larger integration time steps together with the adaptive convergence criteria allowed the computational time of the simulation to be reduced compared with the reference system. The simulation time with the reference solver was about 5 hours, whereas only 147.983 s was spent for the same simulation using the AdvPDS. Moreover, it should be noted that the system with the AdvPDS (in contrast to the use of the classical pseudo-dynamic solver) is numerically stable during the whole 100.5 s of simulation (i.e., the solver kept the same pressure level as the reference system).

B. Circuit 2 simulation

Circuit 2 was simulated for 10 seconds with input signals, which are a constant supply pressure of 14 MPa and voltage signal for the directional control valve that varies from -5 to 8 V with 1 second period. The simulation of the system in the presence of the small volume between the pressure compensator and directional control valve using the reference solver was run with the safe integration time step of 10^{-5} s. Such time step ensured a numerically stable solution for the system.

The adaptive criterion values for the AdvPDS under the condition of trade-off between the accuracy and simulation

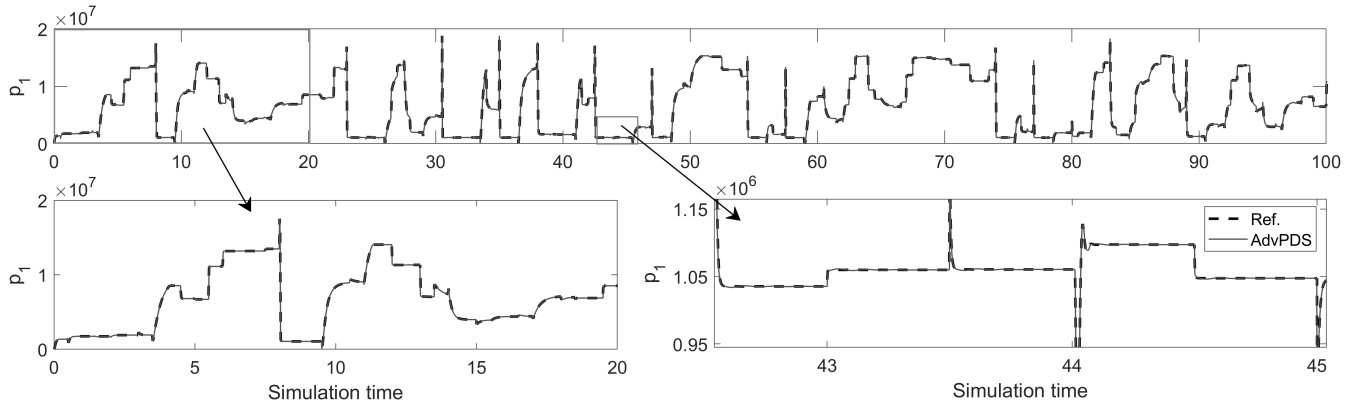

Fig. 10. Pressure responses of Circuit 1 obtained using the reference solver and AdvPDS (with enlarged areas)

time was experimentally chosen using Circuit 1. In order to verify the applicability of the chosen criterion values to other fluid power circuits which also include small volumes Circuit 2 with the AdvPDS was used in another experiment. In the experiment the circuit was simulated 14 times with the different values of the criterion of the AdvPDS while the simulation times and solution accuracy for the cylinder position piston x_p (against the responses obtained with the reference solver) were measured. The use of AdvPDS for the solution of the system allowed the integration time step to be increased to 10^{-4} seconds for both the main and inner loops. The single criteria value was used in order to the dependency (criterion value/accuracy vs. simulation time) showed itself more clearly. The experimental results are summarized in Table III and graphically illustrated by Fig. 11. It can be seen from the figure that the calculation accuracy and simulation time have exponential dependency. Thus, it can be concluded that a larger criterion reduces the simulation time but decrease the calculation accuracy, which is expressed by an increased RMSE. In this case, the criterion equal to 100 can be considered as optimal. However, according to the results, as the increase in overall accuracy was not significant in contrast with the decrease in simulation time, which in our work is the more advantageous system performance. While also taking into account the solution problems in the low-pressure areas, which were solved by use of a smaller criterion, it became clear that the adaptive criteria 300/20 Pa was the most suitable choice. Consequently, the simulation time was 27.572 s, which is a better result compared with the reference system and with systems having a single convergence criterion. The response of the pressure p_3 built up in the small volume as well as the cylinder position piston x_p against the responses obtained with the reference solver can be observed in Fig. 12. The obtained responses of the AdvPDS-based system in pressure and cylinder piston position were accurate and differed from the reference responses with RMSEs of $1.12 \cdot 10^5$ Pa and only $4.24 \cdot 10^{-4}$ m for the pressure and piston position, respectively. The obtained accuracy of the responses was ensured, in particular, by the adaptive criteria, which provided more precise solution in the low-pressure areas. In Table IV, the resulting simulation times for both circuits using reference

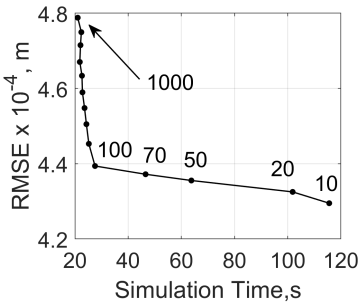

Fig. 11. Dependency between Simulation time and RMSE using AdvPDS with a single criterion value

TABLE III
RELATIONSHIP BETWEEN CRITERIA VALUE, SIMULATION TIME, AND CALCULATION ACCURACY FOR THE ADVPDS WITH A SINGLE CRITERION

Criteria, Pa	Simulation time, s	RMSE $\times 10^{-4}$, m
10	115.593	4.2950
20	101.847	4.3251
50	63.766	4.3554
70	46.558	4.3720
100	27.546	4.3939
200	25.222	4.4529
300	24.307	4.5051
400	23.609	4.5480
500	22.815	4.5897
600	22.638	4.6339
700	21.829	4.6704
800	22.084	4.7151
900	22.400	4.7496
1000	21.043	4.7881

solver and AdvPDS are presented. The appropriateness of the adaptive criterion chosen was confirmed by a number of experiments that were carried out also with Circuit 2.

C. Real-time implementation

To investigate the possibilities of the use of the developed method in real-time and faster than real-time implementations, MATLAB codes for Circuit 2 with the reference solver and the AdvPDS were translated into standalone C code using MATLAB Coder 4.1. Both codes were compiled and run outside MATLAB on a PC with an Intel Core i5-4590 3.30

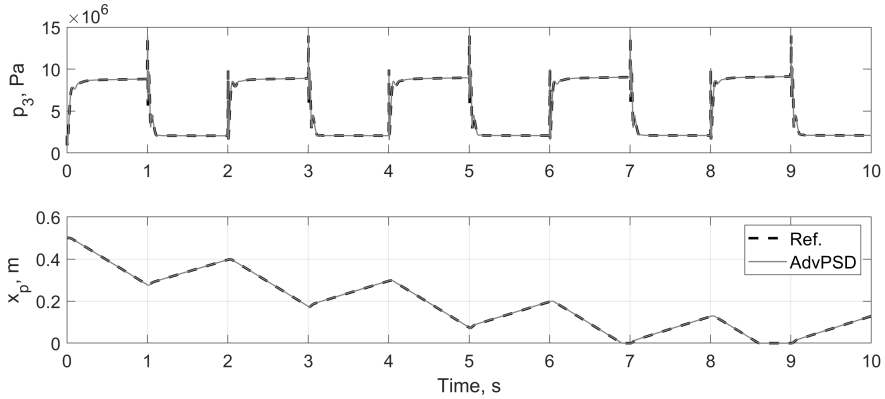

Fig. 12. Circuit 2 responses in pressure p_3 and cylinder piston position x_p using the reference solver and the AdvPDS

TABLE IV
SIMULATION TIME OF CIRCUIT 1 AND CIRCUIT 2 USING THE REFERENCE SOLVER AND THE ADVPDS

Circuit	Solver	Real Time, seconds	Time Step (s) (global/inner)	Simulation Time	Adaptive Criterion	RMSE w.r.t. Ref.
1	Ref.	100.5	$10^{-6}/-$	$\sim$ 5 h	$-$	$-$
	AdvPDS	100.5	$10^{-4}/10^{-5}$	147.983 s	300/10	$RMSE_{p1} = 1.12 \cdot 10^4$ Pa
2	Ref.	10	$10^{-5}/-$	200.350 s	$-$	$-$
	AdvPDS	10	$10^{-4}/10^{-4}$	27.572 s	300/20	$RMSE_{p3} = 1.89 \cdot 10^5$ Pa
						$RMSE_{xp} = 4.24 \cdot 10^{-4}$ m

GHz with 16 GB RAM. As a result, to simulate an interval of 10 s of real time, it took 219 ms for the reference system, whereas for the AdvPDS-based system it took only 47 ms to simulate the same time interval. Thus, the introduction of the developed AdvPDS solver allowed Circuit 2 to be simulated 4.7 times faster in comparison with the use of the reference solver usage. It should be noted that in our case, both implementations were calculated much faster than real-time. However, in virtual prototypes the fluid power system are usually employed in conjunction with mechanical components (i.e., multibody dynamic representation of the mobile machine structure). Thus, the mechanical component should also be calculated at each time step of the real-time simulation. Based on the results, it can be concluded that the use of the AdvPDS for the solution of the real-time and faster than real-time systems, which include fluid power components with the small volumes, can be more beneficial than the reference solver application.

VI. CONCLUSION

In this paper, the advanced pseudo-dynamic solver with adaptive criterion has been proposed for the efficient solution of fluid power systems with singularities originating (in particular) from the presence in the system of small volumes. Based on the results of the experiments performed with two test fluid power circuits, which contained small volumes in their structure, the model for the AdvPDS was formulated. There are two main differences of the AdvPDS in comparison with the classical pseudo-dynamic solver. First, the calculation of the outlet volume flow rate related to the small volume is included into the inner loop of the solver, which allowed the numerical stability of the solution to be increased. Second, the adaptive convergence criterion is introduced, which allowed the simulation time to be decreased and the calculation accuracy to be increased. Side-by-side simulation results confirmed that the proposed solver is much more efficient in solution of the fluid power circuits than the conventional method as well as the classical pseudo-dynamic solver. The main advantage of the proposed solver is that it produces the lower error than the classical pseudo-dynamic solver with single criteria. In addition, the AdvPDS-based model can be calculated faster than the conventional model of the fluid power circuit with small volumes owing to the possibility of the application of a larger integration time step. Moreover, the AdvPDS solver can be the preferable method in modeling of more-detailed fluid power circuits, especially in such cases when the classical pseudo-dynamic solver may show numerically unstable and slow response. The described advantages in solution of the fluid power systems with small volumes of the developed solver allow to use AdvPDS in simulations of mobile machines in the real-time and faster than real-time applications. Moreover, mechatronic applications such as [4], [6], [7] can directly benefit from the usage of the developed solver. In these applications in particular the solver can ensure the accurate real-time or faster than real-time simulation of the multibody systems with the fluid power actuation. Future studies will be associated with the use of the AdvPDS-based fluid power model as a part of the simulation model of a mobile machine for the real-time applications.

REFERENCES

[1] A. Mikkola and H. Handroos, "Modelling and simulation of a flexible hydraulic driven log crane," in *Proceedings of the Ninth Bath International Fluid Power Workshop*, vol. 9-11, September 1996.

[2] S. Esqué, A. Raneda, and A. Ellman, "Techniques for studying a mobile hydraulic crane in virtual reality," *International Journal of Fluid Power*, vol. 4, no. 2, pp. 25–35, 2003.
[3] K. Liu, C. Zhang, and Z. Sun, "Independent pressure and flow rate control enabled by hydraulic free piston engine," *IEEE/ASME Transactions on Mechatronics*, vol. 24, no. 3, pp. 1282–1293, June 2019.
[4] V. Zhidchenko, I. Malysheva, H. Handroos, and A. Kovartsev, "Faster than real-time simulation of mobile crane dynamics using digital twin concept," *Journal of Physics: Conference Series*, vol. 1096, p. 012071, September 2018.
[5] Y. Zheng, T. Ge, and J. Liu, "Kinematics modeling and control simulation for a logging harvester in virtual environments," *Advances in Mechanical Engineering*, vol. 7, no. 10, p. 1687814015611329, 2015.
[6] J. Rahikainen, M. Kiani, J. Sopanen, P. Jalali, and A. Mikkola, "Computationally efficient approach for simulation of multibody and hydraulic dynamics," *Mechanism and Machine Theory*, vol. 130, pp. 435–446, 2018.
[7] I. Malysheva, H. Handroos, V. Zhidchenko, and A. Kovartsev, "Faster than real-time simulation of a hydraulically actuated log crane," in *2018 Global Fluid Power Society PhD Symposium (GFPS)*, 2018, pp. 1–6.
[8] M. M. Pedersen, M. R. Hansen, and M. Ballebye, "Developing a tool point control scheme for a hydraulic crane using interactive real-time dynamic simulation," *Modeling, Identification and Control*, vol. 31, no. 4, pp. 133–143, 2010.
[9] A. Mikkola, "Studies on fatigue damage in a hydraulically driven boom system using virtual prototype simulations," DSc thesis, Lappeenranta University of Technology, Lappeenranta, Finland, 1997.
[10] J. Yao, Z. Jiao, D. Ma, and L. Yan, "High-accuracy tracking control of hydraulic rotary actuators with modeling uncertainties," *IEEE/ASME Transactions on Mechatronics*, vol. 19, no. 2, pp. 633–641, April 2014.
[11] C.-G. Park, S. Yoo, H. Ahn, J. Kim, and D. Shin, "A coupled hydraulic and mechanical system simulation for hydraulic excavators," *Proceedings of the Institution of Mechanical Engineers, Part I: Journal of Systems and Control Engineering*, vol. 234, no. 4, pp. 527–549, 2020.
[12] J. A. Ferreira, F. G. Almeida, M. R. Quintas, and J. P. E. de Oliveira, "Hybrid models for hardware-in-the-loop simulation of hydraulic systems part 2: Experiments," *Proceedings of the Institution of Mechanical Engineers, Part I: Journal of Systems and Control Engineering*, vol. 218, no. 6, pp. 475–486, 2004.
[13] D. E. Bowns and L. M. Wang, "The digital computation of pressures in hydraulic pipes with small volume using an iterative technique," *Proceedings of the Institution of Mechanical Engineers, Part C: Mechanical Engineering Science*, vol. 204, no. 1, pp. 29–36, 1990.
[14] A. Ellman and R. Piché, "A modified orifice flow formula for numerical simulation of fluid power systems," in *Proceedings of the 1996 ASME International Mechanical Engineering Congress and Exposition, Atlanta, Fluid power Systems and Technology*, vol. 3, November 1996, pp. 59–63.
[15] A. Ellman and R. Piché, "A two regime orifice flow formula for numerical simulation," *Journal of Dynamic Systems, Measurements, and Control*, vol. 121, no. 4, pp. 721–724, 1999.
[16] R. Åman, H. Handroos, and T. Eskola, "Computationally efficient two-regime flow orifice model for real-time simulation," *Simulation Modelling Practice and Theory*, vol. 16, no. 8, pp. 945 – 961, 2008, eUROSIM 2007.
[17] E. Hairer and G. Wanner, *Stability Analysis for Explicit RK Methods*. Berlin, Heidelberg: Springer Berlin Heidelberg, 1996, pp. 15–39.
[18] S. Esqué, "A new approach for numerical simulations of fluid power circuits using rosenbrock methods," Ph.D. dissertation, Tampere University of Technology, Tampere, Finland, 2008.
[19] R. Piché and A. Ellman, "Numerical integration of fluid power circuit models using two-stage semi-implicit runge-kutta methods," *Proceedings of the Institution of Mechanical Engineers, Part C: Journal of Mechanical Engineering Science*, vol. 208, no. 3, pp. 167–175, 1994.
[20] R. Åman and H. Handroos, "Pseudo-dynamic solution of pressures in small volumes in fluid power circuit simulation," in *Proceedings of the 5th FPNI PhD Symposium*, July 2008, pp. 406–416.
[21] R. Åman and H. Handroos, "Comparison of numerical effectiveness of three methods for modelling 2-way flow control valves," in *Proceedings of the Seventh International Conference on Fluid Power Transmission and Control*. Beijing World Publishing Corporation, April 2009, pp. 711–715.
[22] R. Åman and H. Handroos, "Optimization of parameters of pseudo-dynamic solver for real-time simulation of fluid power circuits," in *Workshop Proceedings, 7th International Fluid Power Conference Aachen*, vol. 1, March 2010, pp. 495–507.
[23] M. Kiani-Oshtorjani, A. Mikkola, and P. Jalali, "Numerical treatment of singularity in hydraulic circuits using singular perturbation theory," *IEEE/ASME Transactions on Mechatronics*, vol. 24, no. 1, pp. 144–153, February 2019.
[24] J. Rahikainen, "On the dynamic simulation of coupled multibody and hydraulic systems for real-time applications," DSc thesis, Lappeenranta-Lahti University of Technology LUT, Lappeenrata, Finland, 2019.
[25] B. Xu, R. Ding, J. Zhang, L. Sha, and M. Cheng, "Multiphysics-coupled modeling: Simulation of the hydraulic-operating mechanism for a sf6 high-voltage circuit breaker," *IEEE/ASME Transactions on Mechatronics*, vol. 21, no. 1, pp. 379–393, February 2016.
[26] H. E. Merritt, *Hydraulic Control Systems*. Wiley, 1967.
[27] H. Handroos and M. Vilenius, "Flexible semi-empirical models for hydraulic flow control valves," *J Mech Design*, vol. 113, no. 3, pp. 232–238, 1991.
[28] C. Canudas de Wit, H. Olsson, K. J. Åström, and P. Lischinsky, "A new model for control of systems with friction," *IEEE Transactions on Automatic Control*, vol. 40, no. 3, pp. 419–425, March 1995.
[29] H. Olsson, "Control systems with friction," Ph.D. dissertation, Department of Automatic Control, Lund Institute of Technology, Lund, Sweden, 1996.
[30] M. Jelali and A. Kroll, *Hydraulic Servo-systems: Modelling, Identification and Control*, ser. Advances in Industrial Control. Springer-Verlag London, 2002.

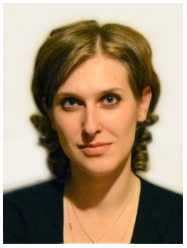

Julia Malysheva received the M. Sc. Degree in 2017 from LUT University, Lappeenranta, Finland within programme in Computational Engineering and Technical Physics with an emphasis in Computer Vision and Pattern Recognition. She is currently working as researcher in Laboratory of Intelligent Machines at LUT University. Her current research focuses on simulation of multibody systems with hydraulic components and deep neural networks.

Stanislav Ustinov received the B. Sc. degree in 2016 from Saimaa University of Applied Sciences, Lappeenranta, Finland within programme in Mechanical Engineering and Production Technology and the M. Sc. degree in 2018 from LUT University, Lappeenranta, Finland within programme in Mechatronic System Design. He is currently working as researcher in Laboratory of Intelligent machines at LUT University. His research interests include fluid power systems, real-time simulation of multibody systems and artificial intelligence.

Heikki Handroos has been a professor of Machine Automation in LUT University since 1993. He earned his M.Sc. and D.Sc. degrees in Tampere University of Technology, 1985 and 1991. His research interests range from mechatronic systems to off-road vehicle transmissions and robotics. He has published about 250 scientific journal and conference papers. He is a member of ASME and IEEE and he has served in several editorial boards of journals and conferences in the field of mechatronics.